Default-Mode Network Disruption in Mild Traumatic Brain Injury[1]

Yongxia Zhou, PhD
Michael P. Milham, MD, PhD[2, 3]
Yvonne W. Lui, MD
Laura Miles, PhD
Joseph Reaume, BSRT
Daniel K. Sodickson, MD, PhD
Robert I. Grossman, MD
Yulin Ge, MD

Purpose: To investigate the integrity of the default-mode network (DMN) by using independent component analysis (ICA) methods in patients shortly after mild traumatic brain injury (MTBI) and healthy control subjects, and to correlate DMN connectivity changes with neurocognitive tests and clinical symptoms.

Materials and Methods: This study was approved by the institutional review board and complied with HIPAA regulations. Twenty-three patients with MTBI who had posttraumatic symptoms shortly after injury (<2 months) and 18 age-matched healthy control subjects were included in this study. Resting-state functional magnetic resonance imaging was performed at 3 T to characterize the DMN by using ICA methods, including a single-participant ICA on the basis of a comprehensive template from core seeds in the posterior cingulate cortex (PCC) and medial prefrontal cortex (MPFC) nodes. ICA *z* images of DMN components were compared between the two groups and correlated with neurocognitive tests and clinical performance in patients by using Pearson and Spearman rank correlation.

Results: When compared with the control subjects, there was significantly reduced connectivity in the PCC and parietal regions and increased frontal connectivity around the MPFC in patients with MTBI ($P < .01$). These fronto-posterior opposing changes within the DMN were significantly correlated ($r = -0.44$, $P = .03$). The reduced posterior connectivity correlated positively with neurocognitive dysfunction (eg, cognitive flexibility), while the increased frontal connectivity correlated negatively with posttraumatic symptoms (ie, depression, anxiety, fatigue, and postconcussion syndrome).

Conclusion: These results showed abnormal DMN connectivity patterns in patients with MTBI, which may provide insight into how neuronal communication and information integration are disrupted among DMN key structures after mild head injury.

[1] From the Center for Biomedical Imaging, Department of Radiology, New York University School of Medicine, 660 First Ave, 4th Floor, New York, NY, 10016 (Y.Z., Y.W.L., L.M., J.R., D.K.S., R.I.G., Y.G.); and Phyllis Green and Randolph Cōwen Institute for Pediatric Neuroscience, New York University Child Study Center, New York, NY (M.P.M.). Received March 30, 2012; revision requested May 15; revision received June 4; accepted June 8; final version accepted June 29. **Address correspondence to** Y.G. (e-mail: *yulin.ge@nyumc.org*).

[2] **Current address:** Center for the Developing Brain, Child Mind Institute, New York, NY

[3] **Current address:** Nathan S. Kline Institute for Psychiatric Research, Orangeburg, NY

Mild traumatic brain injury (MTBI) is a substantial public health problem, representing 75% of traumatic brain injury cases (1). As defined by the World Health Organization (2,3), MTBI results from a traumatic event that causes a brief loss of consciousness, lasting less than 30 minutes, transient memory dysfunction or disorientation that lasts less than 24 hours, or both. Although conventional neuroimaging findings are often normal in patients with MTBI, 20%–30% of individuals develop long-term symptoms, including behavioral, cognitive, and neuropsychologic problems (4), ultimately preventing some from ever successfully reengaging in their normal lives (5). These posttraumatic symptoms, referred to as *postconcussion syndrome* (PCS), manifest as a history of traumatic brain injury along with the presence of three or more common symptoms (ie, headache, dizziness, fatigue, irritability, insomnia, poor concentration, memory difficulty, or an intolerance of stress, emotion, or alcohol) that have lasted at least 3 months (6), as well as evidence of deficits in attention and memory (7). PCS is frequently overlooked at the time of initial injury and can develop and persist for variable periods of time. However, the underlying pathophysiology of PCS is still poorly understood.

In recent years, resting-state functional magnetic resonance (MR) imaging has enabled evaluation of critical brain networks on the basis of baseline energy expenditure in awake and resting states of the brain. Resting-state networks are composed of brain regions with highly correlated time courses of robust low-frequency (<0.1 Hz) blood oxygen level–dependent signal fluctuations (8), which are believed to represent the maintenance of baseline human cognition and metabolic equilibrium (ie, oxygen balance) (9). These intrinsic, spontaneous neuronal activities have been considered to represent important functional architecture for understanding the cognitive functions and can be altered in various neurologic and psychiatric disorders (10). Among these networks, the default-mode network (DMN) is of particular interest. The DMN is a well-established network that is active at rest and suppressed during tasks that require attention and decision making (9,11). The DMN typically comprises the posterior cingulate cortex (PCC), precuneus, inferior parietal, and medial prefrontal cortex (MPFC) nodes (12). Anatomically, the cytoarchitectonic areas of the DMN are suggested to be strongly interconnected (13). Alterations in DMN functional connectivity have been found in several psychiatric disorders (14–17). It is also known that several key cognitive functions are supported by this network (18). For example, the main role of the PCC is memory encoding, consolidation, and environmental monitoring, while the MPFC participates in self-relevance, rapid error identification, and social functions (19). These higher-order cognitive functions are often disrupted in patients with MTBI (20).

Several studies of patients with severe forms of traumatic brain injury, including vegetative states, have shown disrupted DMN connectivity in terms of evaluating patients with consciousness impairment (21–24). Despite considerable interest in the DMN and its relationship with cognitive function, little is known about DMN connectivity changes in MTBI. A recent study by Mayer et al (25) showed decreased connectivity within DMN nodes and increased

Advances in Knowledge

- In patients with mild traumatic brain injury (MTBI), as compared with healthy control subjects, the integrity of default-mode network (DMN) functional connectivity was disrupted, as evidenced by significantly reduced connectivity in the posterior cingulate cortex and parietal regions and increased frontal connectivity around the medial prefrontal cortex ($P < .01$).
- These opposed changes were significantly correlated with each other ($r = -0.44$, $P = .03$), suggesting that frontoposterior DMN nodes are not only intrinsically interdependent but also highly complementary and dynamically equilibratory in their functions after mild injury.
- The reduced posterior connectivity correlated clinically with neurocognitive dysfunction (eg, cognitive flexibility), while the increased frontal connectivity correlated with posttraumatic symptoms (ie, depression, anxiety, fatigue, and postconcussion syndrome [PCS]).

Implication for Patient Care

- Our results of disrupted DMN synchrony and connectivity in MTBI suggest that resting-state functional MR imaging can be used as an additional clinical tool for detecting subtle brain injury that is not apparent with conventional MR imaging and for better understanding the underlying disease pathophysiology of PCS.

Published online
10.1148/radiol.12120748 **Content code:** NR

Radiology 2012; 265:882–892

Abbreviations:
DMN = default-mode network
FSL = Functional Magnetic Resonance Imaging of the Brain Software Library
ICA = independent component analysis
MELODIC = Multivariate Exploratory Linear Optimized Decomposition into Independent Components
MNI = Montreal Neurologic Institute
MPFC = medial prefrontal cortex
MTBI = mild traumatic brain injury
PCC = posterior cingulate cortex
PCS = postconcussion syndrome

Author contributions:
Guarantors of integrity of entire study, Y.W.L., Y.G.; study concepts/study design or data acquisition or data analysis/interpretation, all authors; manuscript drafting or manuscript revision for important intellectual content, all authors; approval of final version of submitted manuscript, all authors; literature research, Y.Z., M.P.M., Y.W.L., R.I.G., Y.G.; clinical studies, Y.Z., L.M., J.R., R.I.G., Y.G.; experimental studies, Y.Z., M.P.M.; statistical analysis, Y.Z., Y.G.; and manuscript editing, Y.Z., M.P.M., Y.W.L., Y.G.

Funding:
This research was supported by the National Institutes of Health (grants R01 NS039135 and NS039135-08S1).

Conflicts of interest are listed at the end of this article.

connectivity between DMN nodes and the lateral prefrontal cortex in MTBI by using seed-based analysis, which is a single time-course correlation approach based on predefined regions of interest. To the best of our knowledge, these findings have not been replicated by using multiple-regression methods, such as independent component analysis (ICA), which is a more robust technique involving the blind source separation method that captures the essential components of multivariate resting-state functional MR imaging data (26). The ICA model is a powerful tool for the extraction of imaging patterns of synchronized neural activity from resting-state functional MR imaging time series. ICA can help separate the whole-brain signal fluctuations from physiologic noise and automatically capture the entire DMN as a single major component (27). This decreases the heterogeneity of DMN patterns when using the seed-based method (28). We hypothesized that there are abnormal neuronal activations of DMN subregions in the resting brain in patients with MTBI, which can be detected with advanced ICA techniques.

To validate our findings, we used three different strategies of ICA, which included a template-based ICA method (29), a hybrid ICA seed-based method (30), and a group ICA method (31) in patients with MTBI compared with healthy individuals. The purpose of this study was to investigate the integrity of the DMN by using ICA methods in patients shortly after MTBI compared with control subjects and to correlate DMN connectivity changes with neurocognitive tests and clinical symptoms.

Materials and Methods

Participants

This institutional review board–approved study was performed between July 2008 and April 2011 and was in compliance with the Health Insurance Portability and Accountability Act. A total of 26 patients with MTBI (recruited from a university-affiliated level 1 trauma center and a university hospital) and 21 healthy control subjects were identified and recruited from a large database in our center of several ongoing neuroimaging projects. All individuals signed a consent form before undergoing MR imaging. All patients experienced a closed head injury with either posttraumatic amnesia of less than 24 hours duration or loss of consciousness of approximately 30 minutes or less, with Glasgow Coma Scale scores between 13 and 15 obtained by the emergency or ambulatory care staff after injury. In this study cohort, all patients experienced loss of consciousness (minimum time of 10 seconds), and all had various posttraumatic symptoms at the time of MR imaging, including headache, insomnia, fatigue, sensitivity to light, irritability, and deficits in attention, memory, and executive function. Exclusion criteria included history of alcohol or drug abuse, neuropsychologic disease before injury, and prior brain injury or other neurologic disease, including stroke, epilepsy, and somatic disorders. On the basis of these criteria, three patients were excluded owing to previous head injury, presence of other neurologic disease, or extensive motion artifacts. Thus, 23 patients with clinically defined MTBI (32) (17 men, six women; mean age, 37.8 years ± 12.9 [standard deviation]; educational attainment, 15 years ± 2.6) were included in this study, with a mean interval of 22 days (range, 3–53 days) between trauma and MR imaging. One control subject was excluded due to an incidental finding of brain lesions at MR imaging, and another two control subjects were excluded due to excessive movement. Eighteen healthy control subjects (mean age, 32.6 years ± 10.0; educational attainment, 16 years ± 2.1) were finally included for comparison, and they were confirmed to have no brain diseases according to patient history and imaging. The two groups had no significant demographic differences in age, sex, or education ($P > .2$).

MR Imaging

MR imaging data were obtained with a 3-T whole-body MR imager (Siemens Tim Trio; Siemens Medical Systems, Erlangen, Germany) by using a 12-channel head coil. Standard gradient-echo echo-planar resting-state functional MR imaging (repetition time msec/echo time msec, 2000/30; flip angle, 75°; field of view, 220 × 220 mm; matrix, 128 × 128; 153 volumes) was performed in the axial plane, parallel to a line through the anterior and posterior commissures (section thickness, 5 mm; section gap, 1 mm) and positioned to cover the entire cerebrum (spatial resolution, 1.72 × 1.72 × 6.00 mm) with an acquisition time of 5 minutes 6 seconds. Individuals were instructed to close their eyes for better relaxation but to stay awake during the imaging protocol. For coregistration and normalization of resting-state functional MR imaging data, three-dimensional T1-weighted magnetization-prepared rapid gradient-echo imaging (repetition time msec/echo time msec/inversion time msec, 2300/2.98/900; flip angle, 9°; resolution, 1 × 1 × 1 mm) was performed. In addition, T2-weighted fast spin-echo and high-spatial-resolution susceptibility-weighted imaging sequences (45/20/900; flip angle, 15°; resolution, 0.5 × 0.5 × 2.0 mm; 52 axial sections) were also implemented to help detect hemorrhagic or other lesions. The conventional T1- and T2-weighted images together with susceptibility-weighted images were reviewed carefully by two experienced radiologists (Y.W.L and Y.G.), and lesions, if present, were documented.

Neuropsychologic Assessment

Neuropsychologic tests were performed within 12 hours of MR imaging for patients with MTBI. The neuropsychologic tests were performed by a psychologist (L.M) who had more than 7 years of experience and was blinded to MR imaging results. Neuropsychologic measures to evaluate cognitive functioning included *(a)* the Symbol Digit Modalities Test (33) to measure information processing speed; *(b)* the Digit Span subtest of the Wechsler Adult Intelligence Scale III (34) to measure verbal attention and concentration, as well as working memory; *(c)* the Trail Making Test A to assess speed and visual attention; *(d)* the Trail Making Test B (35) to assess mental flexibility, specifically the

ability to shift rapidly between cognitive sets; *(e)* the California Verbal Learning Test II to assess verbal learning, as well as immediate and delayed verbal memory (36); and *(f)* the Rey-Osterreith Complex Figure Test to assess visuoperceptual ability and immediate and delayed visual memory (37). These test results were reported in *z* scores. Posttraumatic symptoms, including anxiety, depression, and fatigue, were assessed by using self-report questionnaires and scales, for which higher scores indicate heightened symptoms. The Beck Depression Inventory (38) was used to assess depressive symptoms, fatigue was measured with the Fatigue Severity Scale (39), and subjective symptoms were assessed by using the Postconcussion Symptoms Scale (40). This scale is used to assess the severity of 19 symptoms, such as dizziness, balance problems, headache, and sensitivity to light, which are associated with PCS, mild cognitive impairment, or both. Items are rated on a Likert scale, indicating severity of the symptom, from 0 (none) to 6 (severe). Past research has validated the use of such inventories in the use of assessing individuals after minor head injuries (41).

Image Processing and Data Analysis

All data pre- and postprocessing were performed by an imaging scientist (Y.Z.) with 11 years of experience in functional MR imaging data analysis and interpretation.

Preprocessing.—The three-dimensional magnetization-prepared rapid gradient-echo imaging data were first reoriented, skull stripped, and segmented into gray matter, white matter, and cerebrospinal fluid regions. Thereafter, they were coregistered and normalized to the Montreal Neurologic Institute (MNI) 152-brain template ($2 \times 2 \times 2$ mm). Preprocessing steps for resting-state functional MR imaging data included realignment, spatial Gaussian smoothing with full width at half maximum (6 mm), band-pass temporal filtering of 0.005–0.100 Hz, coregistration to magnetization-prepared rapid gradient-echo imaging and removal of nuisance signals (motion parameters, global signal, and signals derived from cerebrospinal fluid and white matter), and transformation to MNI standard space. The anatomic and functional data were preprocessed by using both the Functional Magnetic Resonance Imaging of the Brain, or FMRIB, Software Library (FSL) (eg, tissue segmentation, registration, smoothing, and regression) and Analysis of Functional NeuroImages, or AFNI, programs (ie, reorientation, skull stripping, motion correction, filtering, and region of interest time courses extraction) (adapted scripts from *http://www.nitrc.org/projects/fcon_1000*).

For correction of motion artifacts, head movement–constraint headphones and a cushion were used to prevent movement during imaging, and all individuals were instructed to keep still during the imaging protocol. AFNI motion-correction algorithms were used to perform more realignment steps with three angular rotation (roll, pitch, and yaw in units of degrees) and three directional displacement (in millimeters) adjustments to further minimize motion artifacts. After these correction steps, no statistical differences were observed in *(a)* the previous six motion parameters and *(b)* frame displacement (42) along all temporal frames between MTBI and control groups ($P > .05$). Additionally, with the ICA approach, movement artifacts can be identified easily and removed separately by applying a band-pass filter.

Seed-based analysis.—After preprocessing, the Pearson correlation coefficient was computed and *z* transformed between the averaged time series of either the PCC- or the MPFC-centered seed and the time course of each voxel in the brain. Two regions of interest, including the MPFC seed (MNI: 0, 48, −3 mm) and the PCC seed (MNI: −6, −48, 39 mm), both with 896-mm^3 volumes, were derived from the script seed library and were well evaluated previously by Fox and Raichle (18). Since the individual seeding approach with the seed placed within either the PCC or the MPFC generates different and incomplete DMN connectivity patterns (43), the combined template from these two DMNs was used and converted into a binary image after applying a threshold of correction of $P < .05$ for subsequent single-participant ICA. The overlap similarity index between PCC- and MPFC-seeding DMN group patterns was calculated as the Dice coefficient, defined as twice the intersection over the sum of cardinalities (44,45). The total number of voxels *(N)* and average correlational *z* value were computed from the obtained entire, anterior, or posterior DMN connectivity maps by using a threshold of correction of $P < .05$. The anterior and posterior portions of the DMN were defined according to MNI coordinates as $y \geq 0$ and $y < 0$, respectively.

Single-participant ICA.—The conventional single-participant ICA was implemented by using information maximization criteria (46) to decompose the data from each individual into 16 spatially statistically independent and intrinsically connected components (47) (*http://cnl.salk.edu/~tewon/ica_cnl.html*). Each component was shown by a *z* score map by subtracting the global mean from each voxel and dividing by the global standard deviation with a threshold of 1.96 (equivalent $P < .05$). After excluding very-low-frequency (<0.01 Hz) or high-frequency (>0.1 Hz) artifacts due to imager drift and cardiac and respiratory motion by applying a band-pass filter, the component that had the maximum difference was chosen to identify the DMN component (C_{DMN}) and generate a *z*-score map by using the following equation:

$$C_{DMN} = \max_i \left\{ C_{i\{T\}} - C_{i\{1-T\}} \right\} \qquad (1)$$

where *i* represents the *i*th low-frequency component, *T* stands for the placement of voxels within the binarized DMN template image generated from the previous seed-based method; $(1 - T)$ represents the region outside the DMN template; and C_i is the average *z* score of the *i*th component inside or outside the template region.

Hybrid ICA.—The DMN detected automatically by means of single-participant ICA was used as a new seed to iterate for the next-round ICA

Figure 1

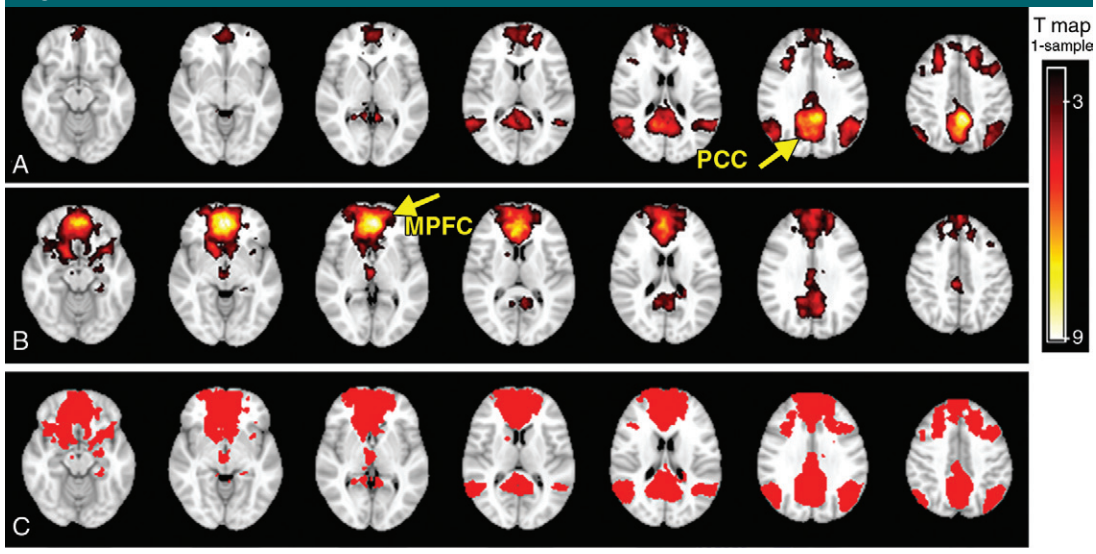

Figure 1: DMN templates created with the seed-based method in healthy control subjects. *A,* PCC-seed–based template, with predominant PCC, bilateral inferior parietal, and MPFC connectivity (corrected, $P < .05$; cluster size, $K \geq 20$). *B,* MPFC-seed–based template shows predominant MPFC connectivity with PCC nodes detected (corrected, $P < .05$; cluster size, $K \geq 20$). *C,* Binarized image of combined-network seeding from the MPFC and PCC show a more inclusive connectivity pattern of the DMN.

template, which is termed "hybrid ICA seed-based method," as proposed by Kelly et al (30). By deriving seed information from single-participant ICA, this hybrid algorithm uses the exploratory power of single-participant ICA to increase the confidence of automatic detection of spatial relationships and to reduce possible original simple seed-template–matching errors. The hybrid ICA is particularly useful in cases where seed-based functional connectivity MR imaging maps would otherwise be generated from seed voxels where multiple components overlap, which is often the case with DMN.

Group ICA.—To validate the single-participant ICA results, group ICA with the FSL Multivariate Exploratory Linear Optimized Decomposition into Independent Components (MELODIC) algorithm *(http://www.fmrib.ox.ac.uk/fsl/melodic/index.html)* (31) was also implemented. The final DMN component of each group was identified with visual inspection on the basis of periodic temporal fluctuation, spatial pattern, and distinct peak of power spectrum at low-frequency (<0.1 Hz) range.

Statistical Analysis

For seed-based analysis, a two-sample *t* test for comparing the voxel numbers or mean *z* values was performed between the patients and control subjects. The FSL FMRIB Local Analysis of Mixed Effects with Ordinary Least Square option (FLAMEO) command was used to analyze the variance of DMN maps within each group and between two groups with corrected $P < .05$. For single-participant ICA, one- and two-sample *t* tests were implemented by applying SPM8 software (Statistical Parametric Mapping, *http://fsl.fmrib.ox.ac.uk/fsl/fslwiki/*) to the *z* image of the DMN made up of ICA components from the two participant groups to generate statistical maps. An integrated threshold was used at a significance level of $P < .01$ and a cluster size of at least 20 voxels for small-volume correction to the whole brain to remove false-positive error and maintain true-positive sensitivity (48). Multiple-comparison corrections at the cluster level were performed on the whole brain on the basis of Gaussian random field theory by using FSL easythresh (minimum, $z > 2.3$; cluster significance, $P < .05$, corrected).

Neuropsychologic measurements were input as covariants for second-level covariance analysis, and Pearson or Spearman rank correlations were performed between either the neurocognitive tests or posttraumatic symptoms (ie, anxiety, depression, fatigue, and PCS) scales and the ICA *z* images of DMN. Bonferroni corrections were performed in patients with a total correction factor of 12 for multiple tests ($n = 6$), and two averaged *z* values ($n = 2$) were obtained from either decreased or increased regions (49).

Results

In the healthy control group, different spatial distribution patterns of DMN were shown when the seed was placed in the standard MPFC versus PCC region, which showed anterior-predominant connectivity with MPFC seeding and posterior-predominant connectivity with PCC seeding (Fig 1, *A* and *B*) (one-sample *t* test with corrected $P < .05$ and cluster size of $K \geq 20$), suggesting an intrinsic region-dependent blood oxygen level–dependent signal coherence of resting-state

networks. The total number of DMN voxels in the healthy control group with PCC seed (n = 16877) had only a 41.2% (DICE coefficient) overlap with MPFC seed (n = 20152). A combined DMN (n = 29397) from both PCC and MPFC seeds was shown to represent a more comprehensive network (Fig 1, *C*) for selecting ICA components. In the control group, this combined DMN showed a more inclusive network pattern (74.2% and 45.9% increase from a PCC- and MPFC-seed–only resting-state network, respectively) involving PCC, precuneus, MPFC, and bilateral parietal regions. By means of visual inspection, patients showed decreased connectivity in the parietal region (PCC seeding), whereas increased connectivity was observed in the frontal region (MPFC seeding) when compared with control subjects. However, such differences did not reach statistical significance (two-sample t test) regarding the voxel numbers of DMN or average z values.

No hemorrhagic brain lesions were detected with conventional imaging, including T2-weighted MR imaging and susceptibility-weighted MR imaging in patients with MTBI. By using a combined DMN template (a binarized image) from both core seeds, single-participant ICA (one-sample t test, $P <$ .01; cluster size, $K \geq 20$) showed a similar spatial connectivity pattern of DMN with seed-based analysis in healthy control subjects (Fig 2, *A*). In patients with MTBI, there was a significantly different distribution pattern of DMN connectivity (Fig 2, *B*) when compared with that of healthy control subjects. Figure 2, *C*, shows comparison results between the two groups (two-sample t test, $P <$ .01), demonstrating significantly increased connectivity primarily in the anterior MPFC region (Table 1) and decreased connectivity primarily in the posterior medial PCC and parietal regions (Table 2) within the DMN in patients with MTBI. Specifically, the increased connectivity in the anterior DMN regions includes the left caudate nucleus, the bilateral medial prefrontal cortex, and the right superior temporal pole, whereas the decreased connectivity in the posterior DMN regions includes the left calcarine cortex (V1), the left posterior cingulate cortex, and the bilateral cuneus. In patients with MTBI, such increased connectivity in the frontal (anterior) regions significantly correlated with decreased connectivity in the posterior regions (r = −0.44, P = .03) (Fig 3), suggesting that these opposite within-network changes are essentially associated.

Figure 2

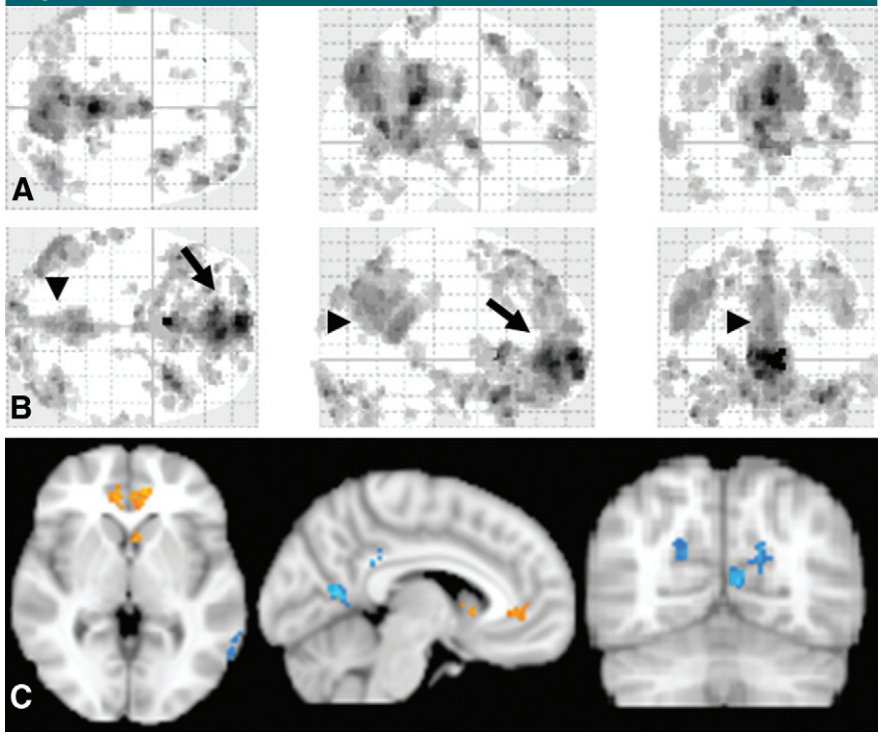

Figure 2: Group t test maps of single-subject ICA results and comparison between patients with MTBI and control subjects. When compared with DMN patterns in the control group *(A),* the patient group *(B)* showed significantly decreased connectivity in the posterior portion (arrowheads) and increased connectivity in the anterior portion (arrows) of the DMN ($P <$ .01; cluster size, $K \geq 20$). *C,* The group-level voxelwise image of single-participant DMN pattern comparing MTBI to control groups shows decreased connectivity regions in blue and increased connectivity regions in yellow.

Table 1

Group Comparison of Increased DMN with Single-Subject ICA in Patients with MTBI versus Healthy Control Subjects

Brain Region	Brodmann Area	MNI Coordinates (x, y, and z in mm)	Cluster Size	z Score	P Value
Left caudate nucleus	....	−2, 12, 2	45	3.19	.001
Left MPFC	10	−12, 44, 2	49	3.08	.001*
Right superior temporal pole	38	34, 10, −24	41	3.04	.001
Right medial frontal	10	8, 44, 2	32	2.78	.004*

Note.—Single-subject ICA was based on whole-brain voxelwise analysis, showing regions with increased DMN. $P <$ .01; cluster size, $K \geq 20$.

* Clusters still survived after use of a Gaussian random-field algorithm (eg, FSL easythresh) for multiple-comparison correction at the cluster level (minimum z score > 2.3; cluster significance, $P <$ .05).

Table 2

Group Comparison of Decreased DMN with Single-Subject ICA in Patients with MTBI versus Healthy Control Subjects

Brain Region	Brodmann Area	MNI *x, y, z* Coordinates (mm)	Cluster Size	*z* Score	*P* Value
Left calcarine cortex (V1)	17	−8, −62, 10	42	3.35	<.001*
Left PCC	23	−4, −38, 28	22	3.18	.001
Right cuneus	19	14, −80, 38	78	2.54	.002
Left cuneus/PCC	23	−16, −64, 26	25	2.75	.003*

Note.—Single-subject ICA was based on whole-brain voxelwise analysis, showing regions with decreased DMN. $P < .01$; cluster size, $K \geq 20$.

* Clusters still survived after use of a Gaussian random-field algorithm (eg, FSL easythresh) for multiple-comparison correction at the cluster level (minimum *z* score > 2.3; cluster significance, $P < .05$).

Figure 3

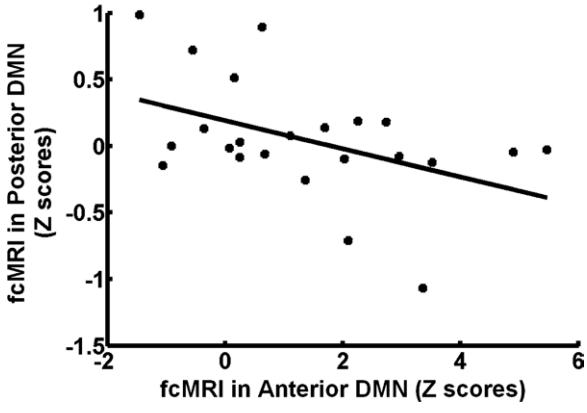

Figure 3: Plot of patients with MTBI shows that increased functional connectivity (*z* scores) in the MPFC region correlates negatively ($r = -0.44$, $P = .03$) with decreased functional connectivity (*z* scores) in the PCC and parietal regions, which may suggest a highly complementary and dynamically equilibratory relationship between the two key substructures of the DMN in terms of function after injury. *fcMRI* = functional connectivity MR imaging.

By using the hybrid ICA seed-based method, we found a similar but augmented pattern of increased frontal connectivity and decreased posterior connectivity of the DMN in patients compared with control subjects (Fig 4). We also performed MELODIC group ICA, the results of which are consistent with single-participant ICA, which showed 43.4% increases of the voxel numbers of the DMN in the anterior regions (MNI coordinate, $y \geq 0$), primarily in the MPFC region, and 24% decreases in the posterior regions (MNI coordinate, $y < 0$) in patients with MTBI compared with control subjects.

In patients with MTBI, there was a significant correlation after Bonferroni correction between decreased DMN in the posterior regions with the Trail Making Test B (Pearson correlation coefficient, $r = 0.60$; corrected, $P = .02$) (Fig 5, *A*), which is a measure of executive functioning to assess mental flexibility—specifically, the ability to shift rapidly between cognitive sets. There was no significant correlation between DMN changes and other neurocognitive tests after Bonforroni adjustment. By using covariance analysis, a significant correlation ($P < .01$) between functional connectivity MR imaging (*z* score) of anterior MPFC and clinical symptoms, including anxiety, depression, fatigue, and postconcussive symptoms, was also found. Figure 5, *B*, shows a representative example of a negative correlation between MPFC connectivity and depression score in patients with MTBI (Spearman correlation coefficient, $r = -0.56$; corrected, $P = .01$), indicating that patients with higher MPFC functional connectivity have a lower degree of depression.

Discussion

Our results show significantly decreased intrinsic functional connectivity in the PCC and parietal regions and increased functional connectivity in the MPFC regions at functional MR imaging in patients shortly after MTBI. We used three different algorithms of ICA to covalidate our findings, and our results are consistent and independent of data processing algorithms, which all suggested posterior hypoconnectivity and anterior hyperconnectivity during the resting state of the brain after injury in patients with MTBI. The observed relationships between DMN disruption and neurocognitive dysfunction, as well as clinical symptoms, provide an additional important clue to the pathophysiology underlying PCS after injury.

Regarding the normal DMN pattern, previous study findings (43,50), together with the current study results in which seed-based methods were used, demonstrated very different connectivity patterns of the DMN in healthy control subjects when the seed was placed separately in PCC versus MPFC regions. For example, Johnson et al reported a dissociation between MPFC and PCC activity by using functional MR imaging during cognitive tasks (51). They provided evidence with task-related functional MR imaging that anterior and posterior regions of the DMN may subserve different functions with respect to different self-reflection conditions. In the current study, we used a comprehensive core-seed–based template for single-participant ICA to select the best fit of coactivation of DMN substructures. The template-based single-participant ICA is a novel automated approach in sorting independent components without subjective identification of the DMN (52,53). By using template-based ICA analysis, Greicius et al also showed improved specificity

Figure 4

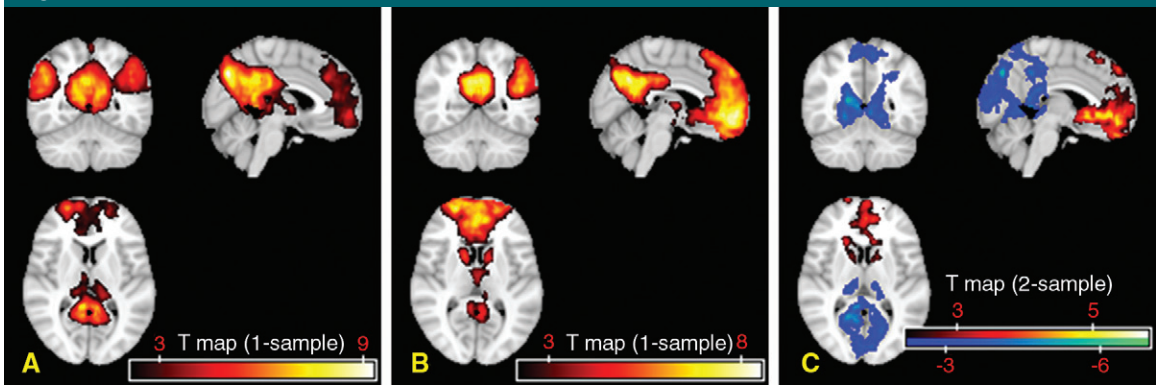

Figure 4: DMN templates obtained with the hybrid ICA seed method in patients and control subjects (corrected, $P < .05$; $K \geq 20$). *A,* Typical but enhanced connectivity pattern of the DMN was identified in the healthy control group. *B,* Disrupted DMN pattern is shown in the patient group. *C,* Group-level voxelwise image of hybrid DMN template differences comparing MTBI to control groups. Red = increased functional connectivity, blue = decreased functional connectivity in patients compared with control subjects. These changes in DMN pattern were consistent with the single-subject ICA results by means of visual inspection.

Figure 5

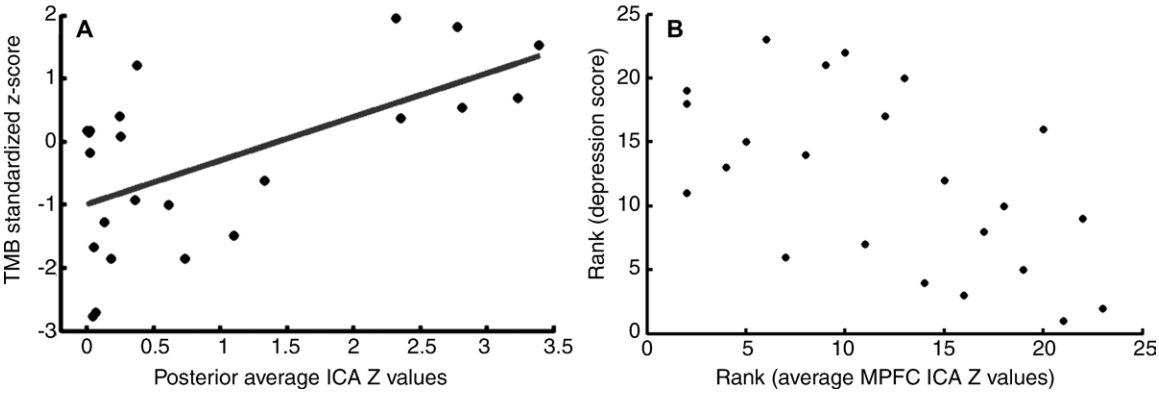

Figure 5: Plots show correlation analyses after Bonferroni correction between neuropsychologic tests and single-subject ICA *z* images in patients with MTBI. *A,* Pearson correlation analysis shows significant positive correlation ($r = 0.60$, $P = .02$) between functional connectivity in posterior regions and Trail Making Test B *z* score. *B,* Spearman rank correlation shows significant negative correlation ($r = -0.56$, $P = .01$) between functional connectivity of the anterior MPFC and depression scores in patients with MTBI.

of detecting DMN abnormalities in patients with Alzheimer disease when the entire template was used, as compared with a PCC-only template (29).

On the basis of single-participant analysis, the regions of decreased functional connectivity within the DMN at functional MR imaging in the present study were found to be predominantly located in the posterior part of the brain, including the cuneus, left calcarine cortex (V1), and PCC. These posterior components of the DMN (eg, the PCC) have been reported to be vulnerable to injury after traumatic brain injury; for example, Yount et al found decreased PCC volume (54) and Levine et al (55) reported that there was gray matter atrophy predominantly involved in the PCC and retrosplenial regions after traumatic brain injury. Relatively recent study findings (24) have implicated DMN connectivity as being reflective of level of consciousness in patients with brain damage. Although the precise role of the DMN in conscious processes remains to be elucidated, all patients with MTBI in the present study experienced a short period of loss of consciousness at the time of trauma. In addition, the reduced posterior functional connectivity of the DMN might indicate subtle axonal pathway injury (56,57). We also found a highly significant correlation between reduced posterior connectivity and decreased cognitive flexibility, as measured with a Trail Making Test B in patients with MTBI, due to the highly involved cognitive processes of this network (20,58,59). Our results of increased MPFC functional connectivity

at functional MR imaging in MTBI may, on the other hand, reflect a compensatory mechanism of increased frontal baseline activity. Increased MPFC activation has been reported previously in moderate and severe traumatic brain injury (60) and is hypothesized to represent brain neuroplasticity operating in recovery and neural repair after injury (61). Our finding of a negative correlation between increased MPFC connectivity and neuropsychologic symptoms also supports the notion of increased usage of MPFC neural resources as compensation in response to the impaired neurocognitive function. Previous studies, outside of traumatic brain injury, have also shown MPFC connectivity changes in patients with anxiety and depression, although the pattern of changes in connectivity appears to be different compared with MTBI (17,62,63). The abnormally increased MPFC usage over the long run, however, might lead to persistent psychologic symptoms, such as the depression, anxiety, and fatigue seen in these patients.

Our finding of a significant negative correlation between increased MPFC functional connectivity and decreased PCC functional connectivity at functional MR imaging in these patients suggests that frontoposterior DMN nodes are not only intrinsically interdependent but also highly complementary in their functions. The within-network discrepant changes have also been identified in other diseases; for example, Zhang et al (53) reported bilaterally decreased MPFC and medial temporal lobe connectivity and increased PCC connectivity in patients with epilepsy, suggesting that DMN components can have distinct alteration patterns with different pathologic circumstances. Jones et al also found increased anterior DMN connectivity and decreased posterior DMN connectivity in aging populations and those with Alzheimer disease (64). These studies support the notion that DMN cannot be considered a homogeneous entity but instead comprises several nodes that serve different, highly complex cognitive functions that are independent but are maintained in a dynamic equilibrium (65). Thus, the functional connectivity and interaction between the MPFC and PCC, which was considered a robust, converged ventral-dorsal compartment model (28), appears to be critical when these structures are injured.

When compared with single-participant ICA, the results of our hybrid ICA seed-based method by using an iterative ICA algorithm showed similar but enhanced patterns of DMN changes in MTBI, providing more converged information about spatial relationships with less heterogeneity and reproducibility problems. In line with the previous two methods, our group ICA, in which we used the FSL MELODIC algorithm on the basis of temporal concatenations of all individuals within each group, also showed increased frontal MPFC connectivity and decreased posterior connectivity around the PCC in patients with MTBI compared with healthy control subjects. Although group ICA is a robust measure (66), it is limited by its inapplicability in individual quantification and correlation with clinical measures. Although our seed-based method did not show statistical significance between patients with MTBI and control subjects when we used the significance level of corrected $P < .05$, the direct visual inspection of seed-based results indeed revealed a similar pattern of differences as when ICA approaches were used. Currently, the seed-based approach is known to have limitations of noise and high dependence on seed location (67,68). By using a seed-based method, Mayer et al (25) showed decreased anterior and posterior functional connectivity within the DMN at functional MR imaging. This discrepancy in findings is likely due to several factors, including the following: *(a)* Their seed-based method was based on interregional correlation between averaged time courses of two specific regions instead of global voxel-wise correlation between time courses of each voxel and template, as used in the current study. *(b)* The PCC seed in their study was chosen to be smaller (679 mm^3) and more anteriorly centered (at MNI coordinates 0, −47, 33) when compared with our seed (896 mm^3, centered at −6, −48, 39). *(c)* There were differences in the interval time between injury and MR imaging, with a mean of 11.5 days postinjury in their study versus 22 days in our study.

A few potential limitations of the current study should be considered. First, this study was limited in scope to the DMN, a most reliable and robust network that supports the "default mode of brain function" during rest. The functional connectivity MR imaging abnormalities of other networks have not been investigated in the current study, and only the thalamic network was reported on previously in MTBI (69). Second, the difference between patients and control subjects with a seed-based method did not reach statistical significance, which raises cautions for the interpretation of our ICA-based findings, despite the fact that the patterns based on the two methods are similar by means of visual inspection. One possibility is that the sample size is relatively small in our groups, which warrants further investigation in a larger population. Third, the results of disrupted DMN connectivity can be caused by structural connectivity abnormalities (eg, axonal injury), which were not investigated in the current study. Future studies designed to explore the relationship between structural and functional network deficits within DMN nodes will be valuable.

Given the important role of the DMN in brain cognitive function, our results of significant changes of DMN functional connectivity in patients with MTBI may provide insights into the underlying mechanisms of the reduced performance in neurocognitive testing. Longitudinal studies are warranted to further evaluate whether the DMN can serve as a biomarker to monitor disease progression and recovery in MTBI.

Acknowledgments: The authors thank Kelly-Anne McGorty, BS, RT, for technical support and Damon Kenul, BS, for manuscript preparation.

Disclosures of Conflicts of Interest: Y.Z. No relevant conflicts of interest to disclose. **M.P.M.** No relevant conflicts of interest to disclose. **Y.W.L.** No relevant conflicts of interest to disclose. **L.M.** No relevant conflicts of interest to disclose. **J.R.**

No relevant conflicts of interest to disclose. **D.K.S.** No relevant conflicts of interest to disclose. **R.I.G.** No relevant conflicts of interest to disclose. **Y.G.** No relevant conflicts of interest to disclose.

References

1. Sosin DM, Sniezek JE, Thurman DJ. Incidence of mild and moderate brain injury in the United States, 1991. Brain Inj 1996;10(1):47–54.
2. Cassidy JD, Carroll LJ, Peloso PM, et al. Incidence, risk factors and prevention of mild traumatic brain injury: results of the WHO Collaborating Centre Task Force on Mild Traumatic Brain Injury. J Rehabil Med 2004;(43 Suppl):28–60.
3. Carroll LJ, Cassidy JD, Peloso PM, et al. Prognosis for mild traumatic brain injury: results of the WHO Collaborating Centre Task Force on Mild Traumatic Brain Injury. J Rehabil Med 2004;(43 Suppl):84–105.
4. Rutland-Brown W, Langlois JA, Thomas KE, Xi YL. Incidence of traumatic brain injury in the United States, 2003. J Head Trauma Rehabil 2006;21(6):544–548.
5. Silver JM, McAllister TW, Yudofsky SC. Textbook of traumatic brain injury. 2nd ed. Washington, DC: American Psychiatric Publishing, 2011.
6. World Health Organization. International Classification of Diseases and Related Health Problems. 10th ed. Geneva, Switzerland: World Health Organization, 2007.
7. American Psychiatric Association. Diagnostic and Statistical Manual of Mental Disorders. 4th ed. Washington, DC: American Psychiatric Association, 2010.
8. Cordes D, Haughton VM, Arfanakis K, et al. Frequencies contributing to functional connectivity in the cerebral cortex in "resting-state" data. AJNR Am J Neuroradiol 2001;22(7):1326–1333.
9. Gusnard DA, Raichle ME, Raichle ME. Searching for a baseline: functional imaging and the resting human brain. Nat Rev Neurosci 2001;2(10):685–694.
10. Zhang D, Raichle ME. Disease and the brain's dark energy. Nat Rev Neurol 2010;6(1):15–28.
11. Shulman GL, Corbetta M, Fiez JA, et al. Searching for activations that generalize over tasks. Hum Brain Mapp 1997;5(4):317–322.
12. Raichle ME, Snyder AZ. A default mode of brain function: a brief history of an evolving idea. Neuroimage 2007;37(4):1083–1090; discussion 1097–1099.
13. Greicius MD, Supekar K, Menon V, Dougherty RF. Resting-state functional connectivity reflects structural connectivity in the default mode network. Cereb Cortex 2009;19(1):72–78.
14. Buckner RL, Andrews-Hanna JR, Schacter DL. The brain's default network: anatomy, function, and relevance to disease. Ann N Y Acad Sci 2008;1124:1–38.
15. Rocca MA, Valsasina P, Absinta M, et al. Default-mode network dysfunction and cognitive impairment in progressive MS. Neurology 2010;74(16):1252–1259.
16. Slobounov SM, Gay M, Zhang K, et al. Alteration of brain functional network at rest and in response to YMCA physical stress test in concussed athletes: RsFMRI study. Neuroimage 2011;55(4):1716–1727.
17. Zhao XH, Wang PJ, Li CB, et al. Altered default mode network activity in patient with anxiety disorders: an fMRI study. Eur J Radiol 2007;63(3):373–378.
18. Fox MD, Raichle ME. Spontaneous fluctuations in brain activity observed with functional magnetic resonance imaging. Nat Rev Neurosci 2007;8(9):700–711.
19. Raichle ME, MacLeod AM, Snyder AZ, Powers WJ, Gusnard DA, Shulman GL. A default mode of brain function. Proc Natl Acad Sci U S A 2001;98(2):676–682.
20. Lux WE. A neuropsychiatric perspective on traumatic brain injury. J Rehabil Res Dev 2007;44(7):951–962.
21. Boly M, Phillips C, Tshibanda L, et al. Intrinsic brain activity in altered states of consciousness: how conscious is the default mode of brain function? Ann N Y Acad Sci 2008;1129:119–129.
22. Hillary FG, Slocomb J, Hills EC, et al. Changes in resting connectivity during recovery from severe traumatic brain injury. Int J Psychophysiol 2011;82(1):115–123.
23. Sharp DJ, Beckmann CF, Greenwood R, et al. Default mode network functional and structural connectivity after traumatic brain injury. Brain 2011;134(Pt 8):2233–2247.
24. Vanhaudenhuyse A, Noirhomme Q, Tshibanda LJ, et al. Default network connectivity reflects the level of consciousness in non-communicative brain-damaged patients. Brain 2010;133(Pt 1):161–171.
25. Mayer AR, Mannell MV, Ling J, Gasparovic C, Yeo RA. Functional connectivity in mild traumatic brain injury. Hum Brain Mapp 2011;32(11):1825–1835.
26. Lee TW, Girolami M, Sejnowski TJ. Independent component analysis using an extended infomax algorithm for mixed subgaussian and supergaussian sources. Neural Comput 1999;11(2):417–441.
27. De Luca M, Beckmann CF, De Stefano N, Matthews PM, Smith SM. fMRI resting state networks define distinct modes of long-distance interactions in the human brain. Neuroimage 2006;29(4):1359–1367.
28. Greicius MD, Krasnow B, Reiss AL, Menon V. Functional connectivity in the resting brain: a network analysis of the default mode hypothesis. Proc Natl Acad Sci U S A 2003;100(1):253–258.
29. Greicius MD, Srivastava G, Reiss AL, Menon V. Default-mode network activity distinguishes Alzheimer's disease from healthy aging: evidence from functional MRI. Proc Natl Acad Sci U S A 2004;101(13):4637–4642.
30. Kelly RE, Wang Z, Alexopoulos GS, et al. Hybrid ICA-seed-based methods for fMRI functional connectivity assessment: a feasibility study. Int J Biomed Imaging 2010;2010. pii: 868976.
31. Beckmann CF, Smith SM. Tensorial extensions of independent component analysis for multisubject FMRI analysis. Neuroimage 2005;25(1):294–311.
32. Petchprapai N, Winkelman C. Mild traumatic brain injury: determinants and subsequent quality of life—a review of the literature. J Neurosci Nurs 2007;39(5):260–272.
33. Smith A. Symbol Digit Modalities Test Manual. Los Angeles, Calif: Western Psychological Services, 1973.
34. Wechsler D. Wechsler Adult Intelligence Scale-III. New York, NY: The Psychological Corporation, 1985.
35. Reitan R. Trail Making Test: Manual for Administration and Scoring. Tucson, Ariz: Reitan Neuropsychology Laboratory, 1992.
36. Delis DC, Kramer JH, Kaplan E, Ober BA. California Verbal Learning Test. Adult Version. Manual. 2nd ed. San Antonio, Tex: The Psychological Corporation, 2000.
37. Meyers JE, Meyers KR. Rey Complex Figure Test and Recognition Trial: Professional manual. Odessa, Fla: Psychological Assessment Resources, 1995.
38. Beck AT, Ward CH, Mendelson M, Mock J, Erbaugh J. An inventory for measuring depression. Arch Gen Psychiatry 1961;4:561–571.
39. Krupp LB, LaRocca NG, Muir-Nash J, Steinberg AD. The fatigue severity scale: application to patients with multiple sclerosis and systemic lupus erythematosus. Arch Neurol 1989;46(10):1121–1123.
40. Aubry M, Cantu R, Dvorak J, et al. Summary and agreement statement of the First International Conference on Concussion in

Sport, Vienna 2001: recommendations for the improvement of safety and health of athletes who may suffer concussive injuries. Br J Sports Med 2002;36(1):6–10.

41. Chen JK, Johnston KM, Collie A, McCrory P, Ptito A. A validation of the post concussion symptom scale in the assessment of complex concussion using cognitive testing and functional MRI. J Neurol Neurosurg Psychiatry 2007;78(11):1231–1238.

42. Power JD, Barnes KA, Snyder AZ, Schlaggar BL, Petersen SE. Spurious but systematic correlations in functional connectivity MRI networks arise from subject motion. Neuroimage 2012;59(3):2142–2154.

43. Uddin LQ, Kelly AM, Biswal BB, Xavier Castellanos F, Milham MP. Functional connectivity of default mode network components: correlation, anticorrelation, and causality. Hum Brain Mapp 2009;30(2):625–637.

44. Dice LR. Measures of the amount of ecologic association between species. Ecology 1945;26(3):297–302.

45. Rombouts SA, Barkhof F, Hoogenraad FG, Sprenger M, Valk J, Scheltens P. Test-retest analysis with functional MR of the activated area in the human visual cortex. AJNR Am J Neuroradiol 1997;18(7):1317–1322.

46. Bell AJ, Sejnowski TJ. An information-maximization approach to blind separation and blind deconvolution. Neural Comput 1995;7(6):1129–1159.

47. Beckmann CF, DeLuca M, Devlin JT, Smith SM. Investigations into resting-state connectivity using independent component analysis. Philos Trans R Soc Lond B Biol Sci 2005;360(1457):1001–1013.

48. Bennett CM, Wolford GL, Miller MB. The principled control of false positives in neuroimaging. Soc Cogn Affect Neurosci 2009;4(4):417–422.

49. Vialatte FB, Cichocki A. Split-test Bonferroni correction for QEEG statistical maps. Biol Cybern 2008;98(4):295–303.

50. Daniels JK, McFarlane AC, Bluhm RL, et al. Switching between executive and default mode networks in posttraumatic stress disorder: alterations in functional connectivity. J Psychiatry Neurosci 2010;35(4):258–266.

51. Johnson MK, Raye CL, Mitchell KJ, Touryan SR, Greene EJ, Nolen-Hoeksema S. Dissociating medial frontal and posterior cingulate activity during self-reflection. Soc Cogn Affect Neurosci 2006;1(1):56–64.

52. Cauda F, Micon BM, Sacco K, et al. Disrupted intrinsic functional connectivity in the vegetative state. J Neurol Neurosurg Psychiatry 2009;80(4):429–431.

53. Zhang Z, Lu G, Zhong Y, et al. Altered spontaneous neuronal activity of the default-mode network in mesial temporal lobe epilepsy. Brain Res 2010;1323:152–160.

54. Yount R, Raschke KA, Biru M, et al. Traumatic brain injury and atrophy of the cingulate gyrus. J Neuropsychiatry Clin Neurosci 2002;14(4):416–423.

55. Levine B, Kovacevic N, Nica EI, et al. The Toronto traumatic brain injury study: injury severity and quantified MRI. Neurology 2008;70(10):771–778.

56. Bazarian JJ, Zhong J, Blyth B, Zhu T, Kavcic V, Peterson D. Diffusion tensor imaging detects clinically important axonal damage after mild traumatic brain injury: a pilot study. J Neurotrauma 2007;24(9):1447–1459.

57. Inglese M, Makani S, Johnson G, et al. Diffuse axonal injury in mild traumatic brain injury: a diffusion tensor imaging study. J Neurosurg 2005;103(2):298–303.

58. Cicerone KD. Remediation of "working attention" in mild traumatic brain injury. Brain Inj 2002;16(3):185–195.

59. Halterman CI, Langan J, Drew A, et al. Tracking the recovery of visuospatial attention deficits in mild traumatic brain injury. Brain 2006;129(Pt 3):747–753.

60. Christodoulou C, DeLuca J, Ricker JH, et al. Functional magnetic resonance imaging of working memory impairment after traumatic brain injury. J Neurol Neurosurg Psychiatry 2001;71(2):161–168.

61. Scheibel RS, Newsome MR, Steinberg JL, et al. Altered brain activation during cognitive control in patients with moderate to severe traumatic brain injury. Neurorehabil Neural Repair 2007;21(1):36–45.

62. Broyd SJ, Demanuele C, Debener S, Helps SK, James CJ, Sonuga-Barke EJ. Default-mode brain dysfunction in mental disorders: a systematic review. Neurosci Biobehav Rev 2009;33(3):279–296.

63. Greicius MD, Flores BH, Menon V, et al. Resting-state functional connectivity in major depression: abnormally increased contributions from subgenual cingulate cortex and thalamus. Biol Psychiatry 2007;62(5):429–437.

64. Jones DT, Machulda MM, Vemuri P, et al. Age-related changes in the default mode network are more advanced in Alzheimer disease. Neurology 2011;77(16):1524–1531.

65. Andrews-Hanna JR, Reidler JS, Sepulcre J, Poulin R, Buckner RL. Functional-anatomic fractionation of the brain's default network. Neuron 2010;65(4):550–562.

66. Zuo XN, Kelly C, Adelstein JS, Klein DF, Castellanos FX, Milham MP. Reliable intrinsic connectivity networks: test-retest evaluation using ICA and dual regression approach. Neuroimage 2010;49(3):2163–2177.

67. Ma L, Wang B, Chen X, Xiong J. Detecting functional connectivity in the resting brain: a comparison between ICA and CCA. Magn Reson Imaging 2007;25(1):47–56.

68. van de Ven VG, Formisano E, Prvulovic D, Roeder CH, Linden DE. Functional connectivity as revealed by spatial independent component analysis of fMRI measurements during rest. Hum Brain Mapp 2004;22(3):165–178.

69. Tang L, Ge Y, Sodickson DK, et al. Thalamic resting-state functional networks: disruption in patients with mild traumatic brain injury. Radiology 2011;260(3):831–840.